

# QAOA with $N \cdot p \geq 200$

Ruslan Shaydulin and Marco Pistoia

Global Technology Applied Research, JPMorgan Chase, New York

## Abstract

One of the central goals of the DARPA Optimization with Noisy Intermediate-Scale Quantum (ONISQ) program is to implement a hybrid quantum/classical optimization algorithm with high  $N \cdot p$ , where  $N$  is the number of qubits and  $p$  is the number of alternating applications of parameterized quantum operators in the protocol. In this note, we demonstrate the execution of the Quantum Approximate Optimization Algorithm (QAOA) applied to the MaxCut problem on non-planar 3-regular graphs with  $N \cdot p$  of up to 320 on the Quantinuum H1-1 and H2 trapped-ion quantum processors. To the best of our knowledge, this is the highest  $N \cdot p$  demonstrated on hardware to date. Our demonstration highlights the rapid progress of quantum hardware.

## Introduction

The Quantum Approximate Optimization Algorithm (QAOA) [1, 2] is one of the leading candidate algorithms for demonstrating better-than-classical performance on near-term quantum computers. As a consequence, the task of implementing QAOA on hardware has attracted a lot of attention. For example, the central goal of Technical Area 1 of the DARPA ONISQ program is to implement a quantum optimizer with high  $N \cdot p$  [3], with  $N \cdot p > 100$  as the target for Phase 1, and  $N \cdot p > 10,000$  for Phase 2. Here,  $N$  refers to the number of qubits used, while  $p$  is the number of alternating applications of QAOA operators (commonly referred to as QAOA layers). QAOA has also been proposed as a scalable application-centric benchmark for quantum hardware [4].

In this note, we report two sets of experiments. First, we report a successful execution of QAOA with classically-optimized parameters applied to the MaxCut problem on 3-regular graphs with  $N = 20$  and  $p \geq 10$  on the Quantinuum H1-1 trapped-ion quantum processor. We consider an execution with  $p$  layers successful if, for all  $1 \leq p' \leq p$ , the solution quality at  $p'$  is greater than at  $p' - 1$ . For all  $N = 20$  problem instances considered, we observe that the solution quality obtained by the algorithm increases monotonically with  $p$  up to 10. For some instances we observe monotonic improvements for  $p$  as large as 15. Second, we extend the experiments to  $N = 32$  by using QAOA with fixed parameters [5] on the Quantinuum H-2 processor. Due to parameters not being optimized on per-instance basis, we observe less consistent QAOA performance. Still, at  $N = 32$  we observe monotonic improvement of QAOA performance with  $p$  up to 10, giving  $N \cdot p = 320$ . To the best of our knowledge, this is the largest (in terms of  $N \cdot p$ ) QAOA demonstration on gate-model quantum computers to date. We make the executed circuits along with the raw data obtained from hardware publicly available at <https://doi.org/10.5281/zenodo.8338585>.

## Results

**Problem Definition** We consider the MaxCut problem on 3-regular graphs. The goal of MaxCut is to partition the set of nodes  $V$  of a graph  $G = (V, E)$  into two disjoint subsets such that the number of edges in  $E$  spanning both parts is maximized. For a sequence of spins  $z \in \{-1, 1\}^{|V|}$ , the MaxCut objective is given by  $\mathcal{C}(z) = \frac{1}{2} \sum_{(i,j) \in E} (1 - z_i z_j)$ . This objective is encoded on qubits by a diagonal Hamiltonian  $C = \frac{1}{2} \sum_{(i,j) \in E} (1 - Z_i Z_j)$ , where  $Z_k$  is a Pauli  $Z$  acting on qubit  $k$ .

The quantum state prepared by QAOA circuit with  $p$  layers is then given by

$$|\beta, \gamma\rangle = \prod_{l=1}^p e^{-i\beta_l \sum_{j=1}^{|V|} x_j} e^{-i\gamma_l C} |+\rangle^{\otimes |V|},$$

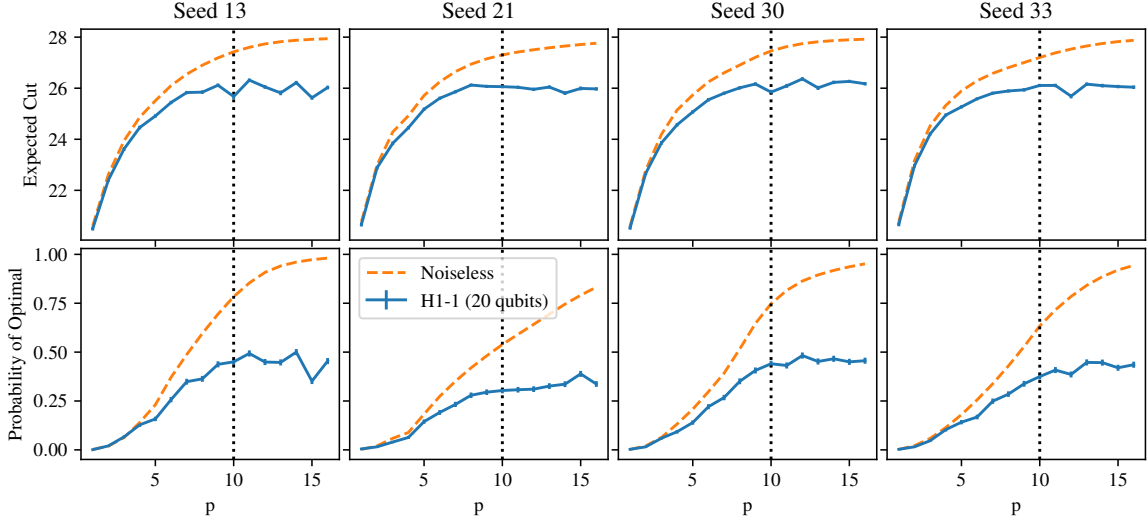


Figure 1: Values of the expected cut  $\langle C \rangle$  (top), and probabilities  $p^{\text{opt}}$  of obtaining the optimal solution (bottom) for all  $N = 20$  instances executed. QAOA parameters are optimized independently for each instance. The optimal cut value for all graphs is 28 and the largest approximation ratio observed on hardware is 0.94. The probability of obtaining the optimal solution increases monotonically for all instances until  $p = 10$  (black vertical dotted line). Error bars show one standard error of the mean.

where  $|+\rangle^{\otimes |V|}$  is a uniform superposition over computational basis states and  $x_j$  is a Pauli  $x$  acting on qubit  $j$ . The central figures of merit are the expected objective value (expected cut in the case of MaxCut), given by

$$\langle C \rangle = \langle \beta, \gamma | C | \beta, \gamma \rangle = \sum_{z \in \{0,1\}^{|V|}} \text{Pr}(z) \mathcal{C}(z),$$

and the probability of obtaining the optimal solution when measuring the QAOA state, denoted as  $p^{\text{opt}}$ . For some instances, we additionally report approximation ratio, given by  $\langle C \rangle / \mathcal{C}^*$ , where  $\mathcal{C}^* = \max_{z \in \{-1,1\}^{|V|}} \mathcal{C}(z)$  is the optimal value of the cut. As can be easily seen, if the parameters are optimized with respect to a given metric, the correspondingly defined solution quality of QAOA can only increase with the number of layers  $p$  in the absence of noise. A noisy device introduces a trade-off between the improvements in solution quality and the increased probability of error from adding more layers. This means that, in practice, there is a depth beyond which adding more layers is not beneficial. In general, this depth is higher if the error rates are lower, motivating the use of  $N \cdot p$  as an application-centric measure of device performance.

**Experimental Setup** The instances are created by generating random 3-regular graphs and post-selecting on the value of optimal cut. For  $N = 28$ , only the instances with optimal cut being at least 28 are included. For higher  $N$ , instances with the largest value of optimal cut found within the sample are picked. We observe that the MaxCut problem for graphs with higher value of optimal cut is harder for QAOA, i.e., higher values of  $p$  are required to approach optimal values of  $\langle C \rangle$  and  $p^{\text{opt}}$ . Consequently, harder instances enable the demonstration of higher  $N \cdot p$ . In Figure 1 and Table 1, each graph is identified by the random seed used to generate it.

For  $N = 20$  instances, we optimize parameters  $\beta, \gamma$  with respect to expected solution quality  $\langle C(\beta, \gamma) \rangle$ . For  $p \leq 11$ , we run one local optimization using COBYLA [6] initialized with fixed-angle parameters [5] obtained from QAOAKit [7]. For  $p > 11$ , we re-parameterize QAOA using the FOURIER scheme [8] with  $q = p$  and run one local optimization using COBYLA [6] initialized with parameters extrapolated from  $p' = p - 1$ . For instances with  $N \geq 24$ , fixed parameters of Ref. [5] are used. The circuit with optimized parameters is compiled into the native gate set of the Quantinuum H1-1 device using the TKET transpiler [9], with each  $z_i z_j$  term in the cost operator  $e^{-i\gamma C}$  implemented using one ZZPhase native two-qubit gate. Therefore, the two-qubit gate count for each circuit is exactly  $p \cdot |E| = 3Np/2$ . We remark that for the trapped-ion architecture of the H1-1 processor, the idling

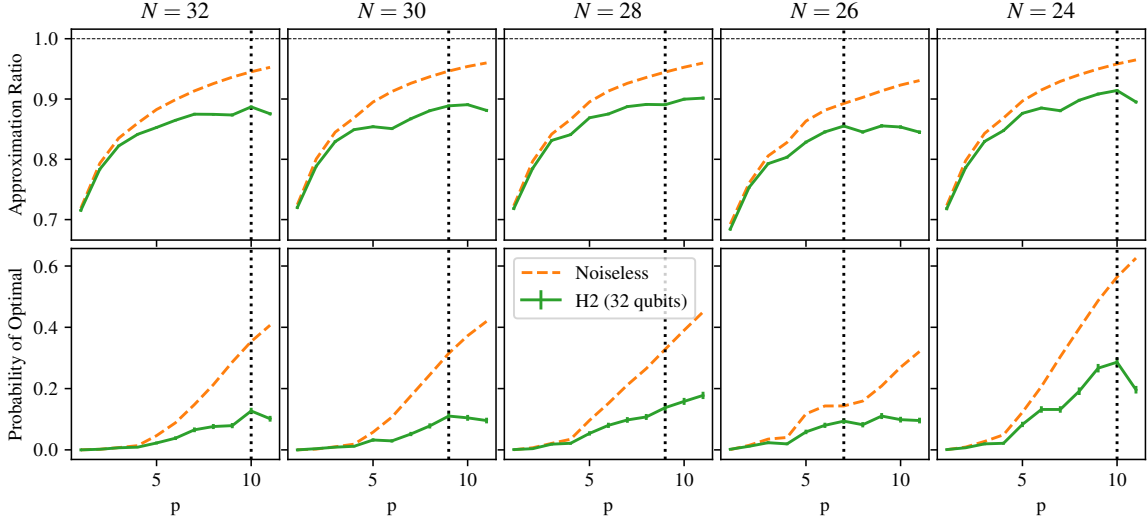


Figure 2: Approximation ratios (top), and probabilities  $p^{\text{opt}}$  of obtaining the optimal solution (bottom) for all  $N \geq 24$  instances executed. Fixed instance-independent QAOA parameters of Ref. [5] are used. Error bars show one standard error of the mean.

and crosstalk errors are low compared to the two-qubit gate errors. Combined with long coherence time, this leads to the success of the circuit execution being defined primarily by the two-qubit gate count, as opposed to the two-qubit gate depth. This is in contrast to superconducting architectures, for which the two-qubit gate depth is more predictive of performance than the two-qubit gate count due to the shorter coherence time and relatively higher crosstalk and idling errors.

**QAOA on the H1-1 and H2 Trapped-Ion Processors** We present the results obtained on the Quantinuum H1-1 quantum processor in Figure 1 and on the H2 in Figure 2. Table 1 lists the complete results for Figure 1 and Table 2 for Figure 2. The executed circuits and the raw data obtained from the device are available at <https://doi.org/10.5281/zenodo.7689982>. We use the probability  $p^{\text{opt}}$  of obtaining the optimal cut as the measure of solution quality for the purposes of defining a “successful execution”.

For  $N = 20$  experiments with instance-specific optimized QAOA parameters, we observe the probability  $p^{\text{opt}}$  of obtaining the optimal cut grows monotonically up to  $p = 10$  that for all four graphs considered. This indicates that the experiments consistently succeed at  $N \cdot p = 200$ , which corresponds to 300 native two-qubit ZZPhase gates. We obtain approximation ratios of up to 0.94. We note that  $p^{\text{opt}}$  continues to grow for higher  $p$  compared to the expected solution quality  $\langle C \rangle$ , which for some instances stops increasing at  $p = 9$ . We conjecture that this difference is due to higher  $p$  required to saturate the success probability in the noiseless case. This conjecture is supported by the observation that the highest  $N \cdot p$  is achieved with instances for which  $p_{\text{ex}}^{\text{opt}}$  grows the slowest. For example, the instance labelled “Seed 21” achieves  $N \cdot p = 300$  and  $p_{\text{ex}}^{\text{opt}} = 0.791$  at  $p = 15$ . In contrast, the same  $p_{\text{ex}}^{\text{opt}}$  is reached at  $p = 11$  for “Seed 13” and “Seed 30”, and  $N \cdot p$  is correspondingly lower.

For  $N \geq 24$  experiments with fixed QAOA parameters, we observe a less consistent performance. For example, for  $N = 32$  the value of  $p^{\text{opt}}$  grows for  $p$  up to 10, whereas for  $N = 26$  the monotonic improvement continues only up to  $p = 7$ . This is due to the fixed QAOA parameters providing non-smooth improvement in  $p^{\text{opt}}$  for  $N = 26$  instance, as evidenced by the exact simulation presented in Fig. 2. To the best of our knowledge, this note reports the largest QAOA execution in terms of  $N \cdot p$  to date. We refer the interested reader to Table 2 in Ref. [10] for an overview of previous state-of-the-art demonstrations. We remark that alternative definitions of QAOA layer may lead to smaller circuits that have higher  $N \cdot p$ . For example, in the recently introduced mixer-phaser ansatz [11], each “layer” can be implemented using only 3 CNOTs. If “layer” is to be redefined in this way, our results indicate that  $N \cdot p \geq 2000$  would become within reach for current hardware. However, in this note we focus on the original QAOA definition.

$p$	$\langle C \rangle_{\text{H1-1}}$	$\langle C \rangle_{\text{ex}}$	$p_{\text{H1-1}}^{\text{opt}}$	$p_{\text{ex}}^{\text{opt}}$	$p$	$\langle C \rangle_{\text{H1-1}}$	$\langle C \rangle_{\text{ex}}$	$p_{\text{H1-1}}^{\text{opt}}$	$p_{\text{ex}}^{\text{opt}}$
1	20.500 $\pm$ 0.073	20.610	0.001 $\pm$ 0.001	0.002	1	20.663 $\pm$ 0.078	20.774	0.005 $\pm$ 0.002	0.002
2	22.405 $\pm$ 0.073	22.620	0.021 $\pm$ 0.004	0.019	2	22.886 $\pm$ 0.073	22.993	0.016 $\pm$ 0.004	0.020
3	23.620 $\pm$ 0.075	23.944	0.066 $\pm$ 0.008	0.063	3	23.843 $\pm$ 0.072	24.286	0.040 $\pm$ 0.006	0.059
4	24.460 $\pm$ 0.074	24.861	0.128 $\pm$ 0.010	0.140	4	24.453 $\pm$ 0.068	24.922	0.063 $\pm$ 0.008	0.089
5	24.913 $\pm$ 0.066	25.512	0.158 $\pm$ 0.011	0.231	5	25.177 $\pm$ 0.066	25.715	0.145 $\pm$ 0.011	0.183
6	25.439 $\pm$ 0.067	26.101	0.257 $\pm$ 0.014	0.371	6	25.606 $\pm$ 0.063	26.249	0.191 $\pm$ 0.012	0.274
7	25.829 $\pm$ 0.066	26.547	0.349 $\pm$ 0.015	0.487	7	25.858 $\pm$ 0.062	26.649	0.232 $\pm$ 0.013	0.351
8	25.846 $\pm$ 0.068	26.900	0.363 $\pm$ 0.015	0.595	8	26.123 $\pm$ 0.059	26.941	0.279 $\pm$ 0.014	0.419
9	26.116 $\pm$ 0.069	27.189	0.438 $\pm$ 0.016	0.694	9	26.071 $\pm$ 0.060	27.150	0.295 $\pm$ 0.014	0.481
10	25.675 $\pm$ 0.097	27.426	0.450 $\pm$ 0.016	0.784	10	26.062 $\pm$ 0.064	27.304	0.304 $\pm$ 0.014	0.539
<b>11</b>	26.316 $\pm$ 0.065	27.601	<b>0.493 <math>\pm</math> 0.016</b>	0.854	11	26.035 $\pm$ 0.064	27.418	0.308 $\pm$ 0.014	0.591
12	26.050 $\pm$ 0.072	27.734	0.449 $\pm$ 0.016	0.908	12	25.956 $\pm$ 0.065	27.506	0.311 $\pm$ 0.014	0.642
13	25.816 $\pm$ 0.091	27.821	0.447 $\pm$ 0.016	0.941	13	26.045 $\pm$ 0.066	27.584	0.326 $\pm$ 0.015	0.694
14	26.219 $\pm$ 0.068	27.878	0.500 $\pm$ 0.016	0.961	14	25.808 $\pm$ 0.073	27.651	0.336 $\pm$ 0.015	0.745
15	25.625 $\pm$ 0.078	27.914	0.352 $\pm$ 0.015	0.973	<b>15</b>	25.990 $\pm$ 0.075	27.710	<b>0.389 <math>\pm</math> 0.015</b>	0.791
16	26.026 $\pm$ 0.071	27.938	0.454 $\pm$ 0.016	0.981	16	25.973 $\pm$ 0.065	27.762	0.337 $\pm$ 0.015	0.832

(a)  $N = 20$ , Seed 13(b)  $N = 20$ , Seed 21

$p$	$\langle C \rangle_{\text{H1-1}}$	$\langle C \rangle_{\text{ex}}$	$p_{\text{H1-1}}^{\text{opt}}$	$p_{\text{ex}}^{\text{opt}}$	$p$	$\langle C \rangle_{\text{H1-1}}$	$\langle C \rangle_{\text{ex}}$	$p_{\text{H1-1}}^{\text{opt}}$	$p_{\text{ex}}^{\text{opt}}$
1	20.537 $\pm$ 0.076	20.610	0.003 $\pm$ 0.002	0.002	1	20.673 $\pm$ 0.080	20.774	0.003 $\pm$ 0.002	0.002
2	22.671 $\pm$ 0.073	22.797	0.016 $\pm$ 0.004	0.020	2	22.963 $\pm$ 0.075	23.167	0.016 $\pm$ 0.004	0.021
3	23.857 $\pm$ 0.072	24.195	0.060 $\pm$ 0.007	0.064	3	24.208 $\pm$ 0.067	24.525	0.047 $\pm$ 0.007	0.059
4	24.568 $\pm$ 0.071	25.146	0.093 $\pm$ 0.009	0.132	4	24.948 $\pm$ 0.063	25.327	0.104 $\pm$ 0.010	0.114
5	25.070 $\pm$ 0.067	25.733	0.140 $\pm$ 0.011	0.208	5	25.269 $\pm$ 0.064	25.894	0.142 $\pm$ 0.011	0.180
6	25.547 $\pm$ 0.066	26.248	0.221 $\pm$ 0.013	0.297	6	25.585 $\pm$ 0.059	26.293	0.168 $\pm$ 0.012	0.256
7	25.803 $\pm$ 0.064	26.604	0.268 $\pm$ 0.014	0.392	7	25.806 $\pm$ 0.060	26.582	0.249 $\pm$ 0.014	0.338
8	26.015 $\pm$ 0.067	26.906	0.351 $\pm$ 0.015	0.516	8	25.892 $\pm$ 0.061	26.806	0.285 $\pm$ 0.014	0.429
9	26.165 $\pm$ 0.065	27.210	0.406 $\pm$ 0.015	0.646	9	25.936 $\pm$ 0.068	27.006	0.338 $\pm$ 0.015	0.528
<b>10</b>	25.847 $\pm$ 0.091	27.459	<b>0.440 <math>\pm</math> 0.016</b>	0.747	10	26.107 $\pm$ 0.063	27.204	0.375 $\pm$ 0.015	0.633
11	26.092 $\pm$ 0.075	27.628	0.432 $\pm$ 0.015	0.816	<b>11</b>	26.108 $\pm$ 0.068	27.384	<b>0.408 <math>\pm</math> 0.015</b>	0.716
12	26.365 $\pm$ 0.066	27.745	0.482 $\pm$ 0.016	0.864	12	25.688 $\pm$ 0.086	27.532	0.386 $\pm$ 0.015	0.784
13	26.013 $\pm$ 0.081	27.818	0.452 $\pm$ 0.016	0.895	13	26.158 $\pm$ 0.066	27.653	0.447 $\pm$ 0.016	0.841
14	26.229 $\pm$ 0.067	27.865	0.466 $\pm$ 0.016	0.918	14	26.100 $\pm$ 0.071	27.751	0.446 $\pm$ 0.016	0.886
15	26.266 $\pm$ 0.064	27.896	0.450 $\pm$ 0.016	0.936	15	26.064 $\pm$ 0.067	27.824	0.420 $\pm$ 0.015	0.920
16	26.175 $\pm$ 0.067	27.919	0.456 $\pm$ 0.016	0.952	16	26.039 $\pm$ 0.068	27.875	0.436 $\pm$ 0.015	0.944

(c)  $N = 20$ , Seed 30(d)  $N = 20$ , Seed 33

Table 1: Expected values of cut ( $\langle C \rangle$ ) and probabilities of obtaining the optimal solution ( $p^{\text{opt}}$ ) with the corresponding standard error of the mean for all  $N = 20$  instances executed on H1-1.  $\langle C \rangle_{\text{ex}}$  and  $p_{\text{ex}}^{\text{opt}}$  are obtained in exact noiseless simulation. Note that for most instances  $p^{\text{opt}}$  continues to improve beyond  $p = 10$ . The last  $p$  for which the  $p^{\text{opt}}$  is still increasing is highlighted in bold.

We further note that neither  $\langle C \rangle$  nor  $p^{\text{opt}}$  measurably decrease as more layers are added. This is in contrast to previous results on superconducting [12, 13] and trapped-ion [14] quantum processors, where at some point additional layers begin to introduce an amount of noise sufficient to significantly decrease the expected solution quality. Combined, these observations suggest that the current experiment is not yet limited by the gate fidelity of the device. Higher values of  $N \cdot p$  may be achieved at current gate fidelities either by considering harder problems (higher  $p$ ) or by loading more ions into the trap (higher  $N$ ).

## Acknowledgements

The authors thank Dylan Herman, Changhao Li, Yue Sun and other members of the Global Technology Applied Research center of JPMorgan Chase for helpful discussions and providing feedback on the manuscript.

## References

- [1] T. Hogg and D. Portnov, “Quantum optimization,” *Information Sciences*, vol. 128, no. 3-4, pp. 181–197, 2000. [Online]. Available: [https://doi.org/10.1016/S0020-0255\(00\)00052-9](https://doi.org/10.1016/S0020-0255(00)00052-9)
- [2] E. Farhi, J. Goldstone, and S. Gutmann, “A quantum approximate optimization algorithm,” *arXiv:1411.4028*, 2014. [Online]. Available: <https://arxiv.org/abs/1411.4028>

$p$	$\langle C \rangle_{H2}$	$\langle C \rangle_{ex}$	$p_{H2}^{opt}$	$p_{ex}^{opt}$	$p$	$\langle C \rangle_{H2}$	$\langle C \rangle_{ex}$	$p_{H2}^{opt}$	$p_{ex}^{opt}$
1	32.910 $\pm$ 0.097	33.071	0.000 $\pm$ 0.000	0.000	1	30.961 $\pm$ 0.097	31.160	0.000 $\pm$ 0.000	0.000
2	36.043 $\pm$ 0.090	36.489	0.002 $\pm$ 0.001	0.002	2	33.915 $\pm$ 0.088	34.424	0.004 $\pm$ 0.002	0.003
3	37.823 $\pm$ 0.088	38.413	0.007 $\pm$ 0.003	0.007	3	35.662 $\pm$ 0.094	36.335	0.009 $\pm$ 0.003	0.010
4	38.705 $\pm$ 0.084	39.556	0.009 $\pm$ 0.003	0.014	4	36.515 $\pm$ 0.082	37.357	0.012 $\pm$ 0.003	0.019
5	39.228 $\pm$ 0.089	40.599	0.022 $\pm$ 0.005	0.046	5	36.725 $\pm$ 0.101	38.486	0.032 $\pm$ 0.006	0.058
6	39.780 $\pm$ 0.091	41.350	0.038 $\pm$ 0.006	0.088	6	36.587 $\pm$ 0.101	39.237	0.029 $\pm$ 0.005	0.107
7	40.242 $\pm$ 0.102	42.018	0.065 $\pm$ 0.008	0.148	7	37.292 $\pm$ 0.102	39.823	0.052 $\pm$ 0.007	0.176
8	40.230 $\pm$ 0.101	42.576	0.076 $\pm$ 0.008	0.213	8	37.865 $\pm$ 0.097	40.289	0.078 $\pm$ 0.008	0.245
9	40.181 $\pm$ 0.111	43.067	0.079 $\pm$ 0.008	0.286	9	38.213 $\pm$ 0.101	40.694	<b>0.110 <math>\pm</math> 0.010</b>	0.315
<b>10</b>	40.800 $\pm$ 0.108	43.478	<b>0.127 <math>\pm</math> 0.010</b>	0.354	10	38.297 $\pm$ 0.101	41.021	0.104 $\pm$ 0.010	0.372
11	40.272 $\pm$ 0.117	43.819	0.102 $\pm$ 0.009	0.407	11	37.887 $\pm$ 0.106	41.275	0.096 $\pm$ 0.009	0.419

(a)  $N = 32$ (b)  $N = 30$ 

$p$	$\langle C \rangle_{H2}$	$\langle C \rangle_{ex}$	$p_{H2}^{opt}$	$p_{ex}^{opt}$	$p$	$\langle C \rangle_{H2}$	$\langle C \rangle_{ex}$	$p_{H2}^{opt}$	$p_{ex}^{opt}$
1	28.734 $\pm$ 0.090	28.916	0.001 $\pm$ 0.001	0.000	1	26.683 $\pm$ 0.088	27.006	0.002 $\pm$ 0.001	0.001
2	31.405 $\pm$ 0.088	31.877	0.004 $\pm$ 0.002	0.007	2	29.394 $\pm$ 0.094	29.668	0.012 $\pm$ 0.003	0.015
3	33.253 $\pm$ 0.086	33.670	0.019 $\pm$ 0.004	0.021	3	30.917 $\pm$ 0.092	31.420	0.023 $\pm$ 0.005	0.035
4	33.635 $\pm$ 0.083	34.644	0.021 $\pm$ 0.005	0.035	4	31.335 $\pm$ 0.088	32.292	0.020 $\pm$ 0.004	0.040
5	34.754 $\pm$ 0.082	35.811	0.054 $\pm$ 0.007	0.096	5	32.312 $\pm$ 0.092	33.672	0.059 $\pm$ 0.007	0.118
6	35.006 $\pm$ 0.086	36.528	0.080 $\pm$ 0.008	0.152	6	32.971 $\pm$ 0.100	34.375	0.080 $\pm$ 0.008	0.143
7	35.495 $\pm$ 0.086	37.042	0.098 $\pm$ 0.009	0.212	7	33.352 $\pm$ 0.094	34.811	<b>0.094 <math>\pm</math> 0.009</b>	0.143
8	35.642 $\pm$ 0.086	37.430	0.107 $\pm$ 0.010	0.265	8	32.966 $\pm$ 0.104	35.204	0.082 $\pm$ 0.009	0.159
<b>9</b>	35.622 $\pm$ 0.099	37.786	<b>0.138 <math>\pm</math> 0.011</b>	0.328	9	33.363 $\pm$ 0.111	35.626	0.110 $\pm$ 0.010	0.209
10	35.989 $\pm$ 0.093	38.110	0.158 $\pm$ 0.011	0.390	10	33.288 $\pm$ 0.110	36.004	0.099 $\pm$ 0.009	0.270
11	36.060 $\pm$ 0.100	38.388	0.178 $\pm$ 0.012	0.450	11	32.954 $\pm$ 0.115	36.295	0.096 $\pm$ 0.009	0.321

(c)  $N = 28$ (d)  $N = 26$ 

$p$	$\langle C \rangle_{H2}$	$\langle C \rangle_{ex}$	$p_{H2}^{opt}$	$p_{ex}^{opt}$
1	24.418 $\pm$ 0.085	24.595	0.001 $\pm$ 0.001	0.001
2	26.734 $\pm$ 0.082	27.122	0.007 $\pm$ 0.003	0.009
3	28.208 $\pm$ 0.078	28.663	0.020 $\pm$ 0.004	0.028
4	28.818 $\pm$ 0.070	29.529	0.021 $\pm$ 0.005	0.049
5	29.794 $\pm$ 0.071	30.489	0.083 $\pm$ 0.009	0.123
6	30.092 $\pm$ 0.075	31.111	0.132 $\pm$ 0.011	0.206
7	29.940 $\pm$ 0.084	31.595	0.132 $\pm$ 0.011	0.304
8	30.530 $\pm$ 0.078	31.968	0.191 $\pm$ 0.012	0.396
9	30.880 $\pm$ 0.082	32.296	0.267 $\pm$ 0.014	0.487
<b>10</b>	31.079 $\pm$ 0.079	32.577	<b>0.286 <math>\pm</math> 0.014</b>	0.564
11	30.434 $\pm$ 0.083	32.806	0.196 $\pm$ 0.012	0.626

(e)  $N = 24$ 

Table 2: Expected values of cut ( $\langle C \rangle$ ) and probabilities of obtaining the optimal solution ( $p^{opt}$ ) with the corresponding standard error of the mean for all  $N \geq 24$  instances executed on H2.  $\langle C \rangle_{ex}$  and  $p_{ex}^{opt}$  are obtained in exact noiseless simulation. Note that for most instances  $p^{opt}$  continues to improve beyond  $p = 10$ . The last  $p$  for which the  $p^{opt}$  is still increasing is highlighted in bold.

- [3] “DARPA Broad Agency Announcement: Optimization with noisy intermediate-scale quantum devices (ONISQ),” Apr 2019. [Online]. Available: <https://www.grants.gov/web/grants/view-opportunity.html?oppId=314702>
- [4] S. Martiel, T. Ayril, and C. Allouche, “Benchmarking quantum coprocessors in an application-centric, hardware-agnostic, and scalable way,” *IEEE Transactions on Quantum Engineering*, vol. 2, pp. 1–11, 2021. [Online]. Available: <https://doi.org/10.1109/tqe.2021.3090207>
- [5] J. Wurtz and D. Lykov, “Fixed-angle conjectures for the quantum approximate optimization algorithm on regular MaxCut graphs,” *Physical Review A*, vol. 104, no. 5, Nov 2021. [Online]. Available: <https://doi.org/10.1103/physreva.104.052419>
- [6] M. J. D. Powell, “A direct search optimization method that models the objective and constraint functions by linear interpolation,” in *Advances in Optimization and Numerical Analysis*. Springer Netherlands, 1994, pp. 51–67. [Online]. Available: [https://doi.org/10.1007/978-94-015-8330-5\\_4](https://doi.org/10.1007/978-94-015-8330-5_4)
- [7] R. Shaydulin, K. Marwaha, J. Wurtz, and P. C. Lotshaw, “QAOAKit: A toolkit for reproducible study, application, and verification of QAOA,” in *Second International Workshop on Quantum Computing Software*, 2021. [Online]. Available: <https://doi.org/10.1109/QCS54837.2021.00011>

- [8] L. Zhou, S.-T. Wang, S. Choi, H. Pichler, and M. D. Lukin, “Quantum approximate optimization algorithm: Performance, mechanism, and implementation on near-term devices,” *Physical Review X*, vol. 10, p. 021067, 2020. [Online]. Available: <https://doi.org/10.1103/PhysRevX.10.021067>
- [9] S. Sivarajah, S. Dilkes, A. Cowtan, W. Simmons, A. Edgington, and R. Duncan, “t|ket): a retargetable compiler for NISQ devices,” *Quantum Science and Technology*, vol. 6, no. 1, p. 014003, Nov 2020. [Online]. Available: <https://doi.org/10.1088/2058-9565/ab8e92>
- [10] P. Niroula, R. Shaydulin, R. Yalovetzky, P. Minssen, D. Herman, S. Hu, and M. Pistoia, “Constrained quantum optimization for extractive summarization on a trapped-ion quantum computer,” *Scientific Reports*, vol. 12, no. 1, Oct 2022. [Online]. Available: <https://doi.org/10.1038/s41598-022-20853-w>
- [11] R. LaRose, E. Rieffel, and D. Venturelli, “Mixer-phaser ansätze for quantum optimization with hard constraints,” *Quantum Machine Intelligence*, vol. 4, no. 2, Jun 2022. [Online]. Available: <https://doi.org/10.1007/s42484-022-00069-x>
- [12] M. P. Harrigan, K. J. Sung, M. Neeley, K. J. Satzinger, F. Arute, K. Arya, J. Atalaya, J. C. Bardin, R. Barends, S. Boixo *et al.*, “Quantum approximate optimization of non-planar graph problems on a planar superconducting processor,” *Nature Physics*, vol. 17, no. 3, pp. 332–336, 2021. [Online]. Available: <https://doi.org/10.1038/s41567-020-01105-y>
- [13] N. Lacroix, C. Hellings, C. K. Andersen, A. Di Paolo, A. Remm, S. Lazar, S. Krinner, G. J. Norris, M. Gabureac, J. Heinsoo, A. Blais, C. Eichler, and A. Wallraff, “Improving the performance of deep quantum optimization algorithms with continuous gate sets,” *PRX Quantum*, vol. 1, p. 110304, Oct 2020. [Online]. Available: <https://doi.org/10.1103/PRXQuantum.1.020304>
- [14] E. Pelofske, A. Bärtshi, J. Golden, and S. Eidenbenz, “High-round QAOA for max  $k$ -SAT on trapped ion NISQ devices,” *arXiv:2306.03238*, 2023. [Online]. Available: <https://arxiv.org/abs/2306.03238>

## Disclaimer

This paper was prepared for informational purposes by the Global Technology Applied Research center of JPMorgan Chase & Co. This paper is not a product of the Research Department of JPMorgan Chase & Co. or its affiliates. Neither JPMorgan Chase & Co. nor any of its affiliates makes any explicit or implied representation or warranty and none of them accept any liability in connection with this paper, including, without limitation, with respect to the completeness, accuracy, or reliability of the information contained herein and the potential legal, compliance, tax, or accounting effects thereof. This document is not intended as investment research or investment advice, or as a recommendation, offer, or solicitation for the purchase or sale of any security, financial instrument, financial product or service, or to be used in any way for evaluating the merits of participating in any transaction.